JOURNAL OF CHEMICAL & ENGINEERING DATA

ARTICLE

pubs.acs.org/jced

Temperature-Induced Transformation of the Phase Diagrams of Ternary Systems $NaBO_2 + NaOH + H_2O$ and $KBO_2 + KOH + H_2O$

Alexei V. Churikov,* Konstantin V. Zapsis, Victor V. Khramkov, Mikhail A. Churikov, and Irina M. Gamayunova

Institute of Chemistry, Saratov State University, 83 Astrakhanskaya Str., Saratov 410012, Russian Federation

ABSTRACT: Concentrated water−alkaline solutions of sodium and potassium borohydrides are used as a fuel and hydrogen source in hydrogen power engineering, including low-temperature fuel cells; borohydrides convert into metaborates. The performance of fuel mixtures is determined by their solubility in water. The solubility in the ternary systems $NaBO_2 + NaOH + H_2O$ and $KBO_2 + KOH + H_2O$ was studied by means of isothermal saturation within the range (−10 to 50) °C. The composition of equilibrium solid phases and those of mixtures corresponding to nonvariant equilibrium points were determined; the solubility diagrams of these systems were constructed. The systems with sodium and potassium ions are considerably different in relation to the temperature influence on the solubility of the solid components. The presence of a range of homogeneous solutions and fields of crystallization of hydrated and anhydrous forms of the metaborates and hydroxides is characteristic for both systems at all investigated temperatures. The composition of crystalline hydrates depends on the component ratio in the mixture and the cation nature.

INTRODUCTION

The present work continues our research reported in ref 1 of solubility in the ternary systems "metaborate + alkali + water". Solutions containing these components are known[2−4] to be formed as a result of discharging of borohydride fuel cells (FC). From the technological viewpoint, the discharged fuel must be liquid because any solid precipitation possibly formed would partially destroy the porous structure of the electrodes and worsen the performance of the FC on the whole. In this connection, searching for proper compositions of the $NaBO_2 + NaOH + H_2O$ and $KBO_2 + KOH + H_2O$ systems, concentrated and homogenized as much as possible, is important, and then, initial fuel compositions can be calculated from those of the discharged fuel.

Early works[5−7] contain data on the binary $NaBO_2 + H_2O$ and $KBO_2 + H_2O$ systems. In our previous paper[1] the solubility in the ternary $NaBO_2 + NaOH + H_2O$ and $KBO_2 + KOH + H_2O$ systems was studied at −10 °C. The phase diagrams are shown to be characterized by the presence of relatively narrow fields of homogeneous solution and many crystallization fields; for example, in the $NaBO_2 + NaOH + H_2O$ system, five solid phases crystallize: ice, $NaBO_2 \cdot 2H_2O$, $NaBO_2 \cdot 4H_2O$, $NaOH \cdot H_2O$, and $NaOH \cdot 4H_2O$. The $KBO_2 + KOH + H_2O$ system is also characterized by five crystallization fields: ice, $KOH \cdot H_2O$, $KBO_2 \cdot 4H_2O$, $KBO_2 \cdot 1.5H_2O$, and $KBO_2 \cdot 1.25H_2O$. As the formation of crystallization phases is determined by temperature, it seems topical to study the solubility in the ternary $NaBO_2 + NaOH + H_2O$ and $KBO_2 + KOH + H_2O$ systems at various temperatures.

In this connection, the present work examines the temperature-induced transformation of the phase diagrams of the ternary $NaBO_2 + NaOH + H_2O$ and $KBO_2 + KOH + H_2O$ systems, the regularities of changes in the compositions of solid phases and mixtures corresponding to nonvariant equilibrium points. Solubility isotherms within a temperature range of (−10 to 50) °C are constructed.

EXPERIMENTAL SECTION

Phase equilibria in mixtures of the components of the ternary $NaBO_2 + NaOH + H_2O$ and $KBO_2 + KOH + H_2O$ systems were studied by thermal saturation of solutions according to the experimental technique described earlier.[1] The isothermal saturation was carried out in a glass vessel 1 with an electric mixer 2, an air fitting pipe 3, a liquid seal 4, and a temperature-controlled jacket 5 of a tube for sampling 6 (Figure 1). The investigated mixture in a quantity of (20 to 40) g was loaded into a vessel 1 through the top tube, and a liquid seal 4 was filled with glycerol for prevention of gaseous exchange with the atmosphere; the electric mixer 2 was inserted. Lateral apertures for sampling were sealed. The bottom half of the vessel with the mixture sits in a thermostat; a process of the isothermal saturation begins after switching on the mixer.

The equilibrium time has been preliminarily determined at the dissolution of $NaBO_2$ and KBO_2 in water at the lowest used temperature, 10 °C. The "concentration−time" dependences during (1 to 7) h of the solution saturation at stirring are presented in Figure 2. A systematic change of the solution concentration is not found through (1 to 2) h of stirring at 10 °C. Hence, equilibrium in the systems is reached quickly enough at 10 °C, and it is reached even more quickly at 25 and 50 °C. Therefore, we used the solution saturation over (2 to 3) h with the subsequent isothermal settling of mixtures during 1 h.

The compositions of solutions and solid precipitations were determined by acid−base titration; the technique of analysis is also described in detail in ref 1. The titration was done with a 0.999 $mol \cdot L^{-1}$ HCl solution. The results of experiments are presented as Gibbs−Roseboom's concentration triangles, whose

Received: July 14, 2010
Accepted: January 3, 2011
Published: January 19, 2011

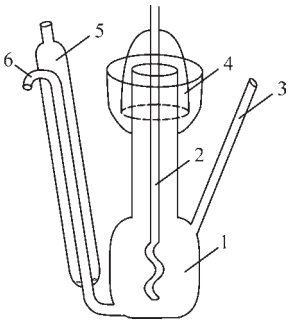

Figure 1. Glass vessel for solubility definition by the method of isothermal saturation. 1, tank for mixture loading; 2, electric mixer; 3, air fitting pipe; 4, liquid seal filled with glycerol; 5, temperature-controlled jacket; 6, tube for sampling.

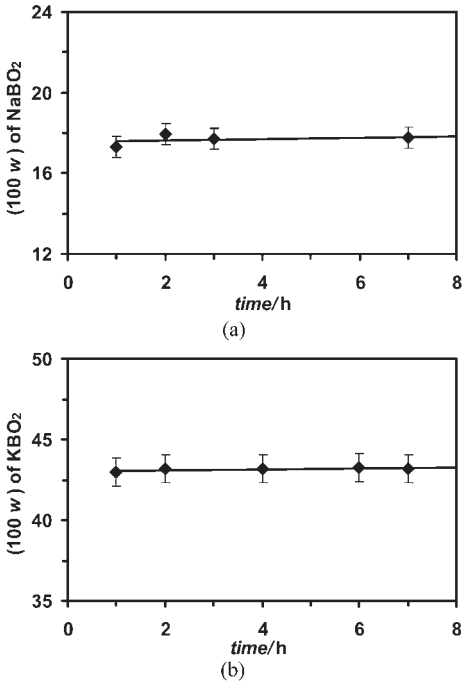

Figure 2. Concentrations of dissolved (a) $NaBO_2$ and (b) KBO_2 as a function of stirring duration at 10 °C.

vertices, points on the sides, and points inside the triangle correspond to the individual components, binary systems, and ternary mixtures, respectively.

The definition of the content of each component in a liquid phase or in a wet solid phase was realized in a three-parallel sampling method with the subsequent averaging and the definition of a standard deviation $s = ((\sum_i (x_i - \bar{x})^2)/(n - 1))^{1/2}$, where x_i is a value of the ith measurement, $\bar{x}$ is an arithmetic mean, and n is the quantity of the parallel samples. The typical result illustrating the experimental repeatability is presented in Table 1.

RESULTS AND DISCUSSION

Figure 3 presents the solubility diagram of the $NaBO_2$ + NaOH + H_2O system at 10 °C; the coordinates of the points corresponding to the composition of equilibrium liquid and solid phases are given in Table 2. The area of the liquid phase l is

Table 1. Typical Result of Chemical Analysis of the $NaBO_2$ (1) + NaOH (2) + H_2O (3) System (Temperature 10 °C; Point #19)

	composition of liquid phase (100 w)								
sample number	$NaBO_2$	mean	s	NaOH	mean	s	H_2O	mean	s
1	2.6	2.4	0.3	51.0	51.0	0.1	46.4	46.6	0.3
2	2.0			51.1			46.9		
3	2.6			50.9			46.5		

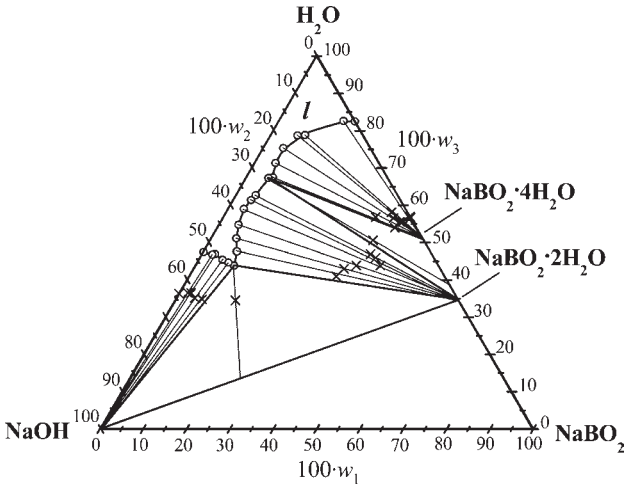

Figure 3. Phase diagram for the $NaBO_2$ (1) + NaOH (2) + H_2O (3) system at 10 °C (l is the area of the liquid phase). Compositions of the equilibrium liquid phase (○) and wet solid phase (+) are listed in Table 2. Thin lines are tie-lines between coexisting phases; thick solid lines are the bounds between monophase, two-phase, and three-phase areas.

limited by the crystallization lines of the solid phases. The solubility of $NaBO_2$ in pure water is $w = 0.177$. A small additive of alkali results in an insignificant increase in the total solubility of components in the system, and the solubility of sodium metaborate reduces; it crystallizes as the tetrahydrate. A further addition of alkali leads to a sharp increase in the total solubility in the system, and the primary crystallizing tetrahydrate $NaBO_2 \cdot 4H_2O$ peritectically breaks down into the dihydrate $NaBO_2 \cdot 2H_2O$ at the peritonic point $p1$. The solubility of $NaBO_2$ decreases down to $w = 0.053$ in the point $p1$ (Table 2). The eutonic point $e1$ corresponds to the equilibrium ($l + S_{NaBO_2 \cdot 2H_2O} + S_{NaOH}$). To the left of the eutonic triangle, there is the crystallization field of NaOH.

An increase in temperature in the system up to 25 °C results in the regular moving of points on the diagram and reduction of the crystallization fields (Figure 4). The set of solid phases in the system does not change ($NaBO_2 \cdot 4H_2O$, $NaBO_2 \cdot 2H_2O$, and NaOH), but the total solubility of components in the system somewhat increases. This is evidenced by the displacement of the liquidus and expansion of the homogeneous solution field l on the triangle. The solubility of $NaBO_2$ in the high-alkaline eutonic point $e2$ becomes relatively large at $w_1 = 0.14$. The compositions of the equilibrium liquid and solid phases are given in Table 3.

Let us consider the phase diagram of the $NaBO_2$ + NaOH + H_2O system at 50 °C. The compositions of liquid and solid phases are shown in Table 4, and the diagram is presented in

dx.doi.org/10.1021/je1007422 |J. Chem. Eng. Data 2011, 56, 383–389

Table 2. Equilibrium Data of the $NaBO_2$ (1) + NaOH (2) + H_2O (3) System at 10° C[a]

composition of liquid phase (100 *w*)			composition of wet solid phase (100 *w*)			equilibrium crystalline phase
$NaBO_2$	NaOH	H_2O	$NaBO_2$	NaOH	H_2O	
17.7	0.0	82.3	43.0	0.0	57.0	$NaBO_2 \cdot 4H_2O$
15.0	2.6	82.4	43.3	0.1	56.6	$NaBO_2 \cdot 4H_2O$
6.3	15.2	78.5	38.2	3.7	58.1	$NaBO_2 \cdot 4H_2O$
8.0	13.4	78.6	42.0	2.5	55.5	$NaBO_2 \cdot 4H_2O$
4.7	20.2	75.1	39.4	4.0	56.6	$NaBO_2 \cdot 4H_2O$
4.9	24.0	71.1	35.2	8.0	56.8	$NaBO_2 \cdot 4H_2O$
6.2	26.5	67.3	41.0	5.0	54.0	$NaBO_2 \cdot 4H_2O$
5.3	27.6	67.1	37.7	11.7	50.6	$NaBO_2 \cdot 4H_2O$ + $NaBO_2 \cdot 2H_2O$ (*p*1)
4.6	32.9	62.5	39.0	14.1	46.9	$NaBO_2 \cdot 2H_2O$
4.2	34.6	61.2	40.6	13.4	46.0	$NaBO_2 \cdot 2H_2O$
3.7	37.5	58.8	42.7	13.4	43.9	$NaBO_2 \cdot 2H_2O$
4.6	40.8	54.6	37.2	18.9	43.9	$NaBO_2 \cdot 2H_2O$
5.9	43.2	51.0	34.8	22.2	43.0	$NaBO_2 \cdot 2H_2O$
7.7	44.8	47.5	34.0	25.0	41.0	$NaBO_2 \cdot 2H_2O$
8.9	47.4	43.7	14.0	51.5	34.5	NaOH + $NaBO_2 \cdot 2H_2O$ (*e*1)
7.2	48.3	44.6	6.2	59.0	34.8	NaOH
5.4	49.3	45.3	4.3	60.5	35.2	NaOH
2.9	50.3	46.8	2.8	60.7	36.5	NaOH
2.4	51.0	46.6	2.0	61.5	36.5	NaOH
0.0	52.7	47.3	0.0	63.6	36.4	NaOH

[a] Compositions and the equilibrium crystalline phases of peritonic point (*p*1) and eutonic point (*e*1) are underlined.

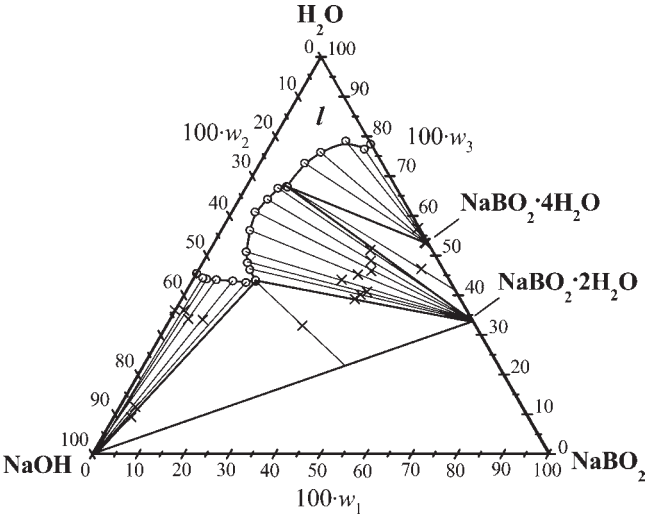

Figure 4. Phase diagram for the $NaBO_2$ (1) + NaOH (2) + H_2O (3) system at 25 °C (*l* is the area of the liquid phase). Compositions of the equilibrium liquid phase (○) and wet solid phase (+) are listed in Table 3. Thin lines are tie-lines between coexisting phases; thick solid lines are the bounds between monophase, two-phase, and three-phase areas.

Figure 5. As is seen, the diagram has essentially changed in comparison with the low-temperature isotherms. The essential

Table 3. Equilibrium Data of the $NaBO_2$ + NaOH + H_2O System at 25 °C[a]

composition of liquid phase (100 *w*)			composition of wet solid phase (100 *w*)			equilibrium crystalline phase
$NaBO_2$	NaOH	H_2O	$NaBO_2$	NaOH	H_2O	
22.5	0.0	77.5	–	–	–	$NaBO_2 \cdot 4H_2O$
21.3	2.3	76.4	42.7	0.4	56.9	$NaBO_2 \cdot 4H_2O$
16.2	5.4	78.4	–	–	–	$NaBO_2 \cdot 4H_2O$
12.0	11.6	76.4	46.3	0.7	53.0	$NaBO_2 \cdot 4H_2O$
9.6	16.5	73.9	46.0	0.8	53.2	$NaBO_2 \cdot 4H_2O$
8.5	23.8	67.7	48.6	4.8	46.6	$NaBO_2 \cdot 4H_2O$ + $NaBO_2 \cdot 2H_2O$ (*p*2)
7.2	25.8	67.0	35.1	13.6	51.3	$NaBO_2 \cdot 2H_2O$
6.1	29.7	64.2	36.6	14.7	48.7	$NaBO_2 \cdot 2H_2O$
4.9	33.8	61.3	37.9	16.0	46.1	$NaBO_2 \cdot 2H_2O$
6.1	37.5	56.4	35.5	19.3	45.2	$NaBO_2 \cdot 2H_2O$
9.3	41.1	49.6	32.6	23.5	43.9	$NaBO_2 \cdot 2H_2O$
11.1	42.4	46.5	38.5	21.3	40.2	$NaBO_2 \cdot 2H_2O$
14.0	43.0	43.0	29.7	38.0	32.3	NaOH + $NaBO_2 \cdot 2H_2O$ (*e*2)
12.2	44.6	43.2	3.5	84.6	11.9	NaOH
8.9	47.7	43.4	7.3	58.9	33.8	NaOH
5.1	51.2	43.7	4.0	62.0	34.0	NaOH
2.9	53.2	43.9	–	–	–	NaOH
1.9	54.0	44.1	2.0	61.8	36.2	NaOH
0.0	54.7	45.3	0.0	63.8	36.2	NaOH

[a] Compositions and the equilibrium crystalline phases of peritonic point (*p*2) and eutonic point (*e*2) are underlined.

increase of the homogeneous field with the concentration of saturated solution $w_{NaBO_2+NaOH} > 0.6$ is a characteristic feature, and displacement of the eutonic point toward the alkaline side of the triangle is observed. Partial recrystallization of solid phases and the formation of new phases is another distinctive feature of the system at 50 °C. Schreinemakers' ray construction has allowed us to reveal the existence of four solid phases (the crystalline hydrates $NaBO_2 \cdot 2H_2O$, $NaBO_2 \cdot 0.5H_2O$, and the anhydrous components NaOH and $NaBO_2$). The eutonic point *e*3 corresponds to the equilibrium of a saturated solution and solid anhydrous components ($l + S_{NaBO_2} + S_{NaOH}$). This diagram has appeared the most difficult for studying since the saturated solutions were viscous, syrupy, and hardly separated from a solid because of high concentration of the dissolved substances.

Some natural transformation of the phase diagram occurs at the 10 °C → 25 °C → 50 °C transition. The existence field of the multiwater crystalline hydrate $NaBO_2 \cdot 4H_2O$ reduces at increasing temperature due to the movement of the peritonic point along the liquidus from the eutonic point to the lateral side of the triangle, where it is absorbed (disappear) as the temperature of decay of the corresponding crystalline hydrate in the binary system is achieved. The peritonic point, moving, "drags" the peritonic triangle. For example, the crystallization field of the hydrate $NaBO_2 \cdot 4H_2O$ must completely disappear on approaching its melting temperature (t = 58 °C).[7] Simultaneously, the crystallization fields of the new solid phase $NaBO_2 \cdot 0.5H_2O$ containing less water and the anhydrous salt $NaBO_2$ appear. New peritonic points and peritonic triangles appear, originating from

dx.doi.org/10.1021/je1007422 |*J. Chem. Eng. Data* 2011, 56, 383–389

Table 4. Equilibrium Data of the $NaBO_2$ + NaOH + H_2O System at 50 °C[a]

composition of liquid phase (100 *w*)			composition of wet solid phase (100 *w*)			equilibrium crystalline phase
$NaBO_2$	NaOH	H_2O	$NaBO_2$	NaOH	H_2O	
29.6	8.0	62.4	45.6	4.3	50.1	$NaBO_2 \cdot 2H_2O$
23.0	13.9	63.1	–	–	–	$NaBO_2 \cdot 2H_2O$
19.5	19.0	61.6	49.1	6.4	44.5	$NaBO_2 \cdot 2H_2O$
19.1	20.2	60.7	37.0	11.9	51.1	$NaBO_2 \cdot 2H_2O$
17.7	25.6	56.8	–	–	–	$NaBO_2 \cdot 2H_2O$
18.0	30.4	51.6	–	–	–	$NaBO_2 \cdot 2H_2O$
19.4	33.2	47.4	37.9	19.3	42.8	$NaBO_2 \cdot 2H_2O$
20.5	35.0	44.5	43.9	16.1	40.0	$NaBO_2 \cdot 2H_2O$
22.0	36.0	42.0	39.4	21.1	39.5	$NaBO_2 \cdot 2H_2O$
21.9	36.9	41.2	42.5	21.2	36.3	$NaBO_2 \cdot 2H_2O$ + $NaBO_2 \cdot 0.5H_2O$ (*p*3)
22.0	38.0	40.0	55.3	18.9	25.8	$NaBO_2 \cdot 0.5H_2O$
21.8	39.9	38.3	–	–	–	$NaBO_2 \cdot 0.5H_2O$ + $NaBO_2$ (*p*4)
18.0	43.1	38.9	–	–	–	$NaBO_2$
15.0	47.0	38.0	25.0	41.4	33.6	$NaBO_2$
12.3	52.1	35.6	30.0	41.7	28.3	$NaBO_2$
10.6	56.1	33.3	13.4	60.1	26.5	NaOH + $NaBO_2$ (*e*3)
5.3	59.2	35.5	4.1	64.4	31.5	NaOH
3.6	59.9	36.5	3.3	63.7	33.0	NaOH
2.5	59.9	37.6	2.3	66.6	31.1	NaOH
0.0	60.9	39.1	0.0	64.9	35.1	NaOH

[a] Compositions and the equilibrium crystalline phases of peritonic points (*p*3, *p*4) and eutonic point (*e*3) are underlined.

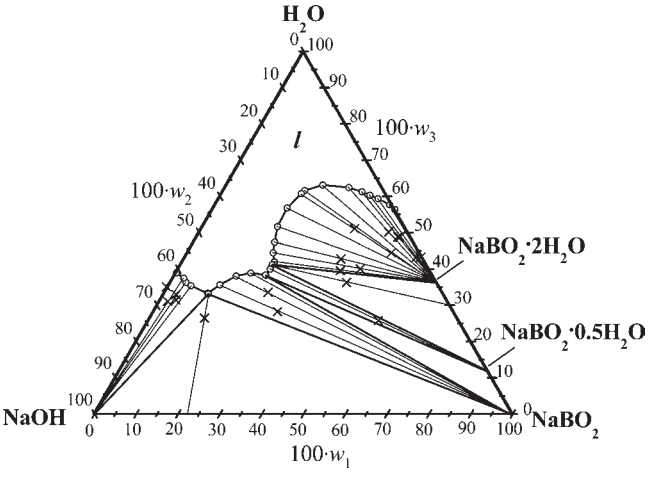

Figure 5. Phase diagram for the $NaBO_2$ (1) + NaOH (2) + H_2O (3) system at 50 °C (*l* is the area of the liquid phase). Compositions of equilibrium liquid phase (○) and wet solid phase (+) are listed in Table 4. Thin lines are tie-lines between coexisting phases; thick solid lines are the bounds between monophase, two-phase, and three-phase areas.

the eutectic point and also moving, at increasing temperature, from the diagram's center toward its lateral sides. Figure 6 demonstrates the movement of the lines of saturated solutions

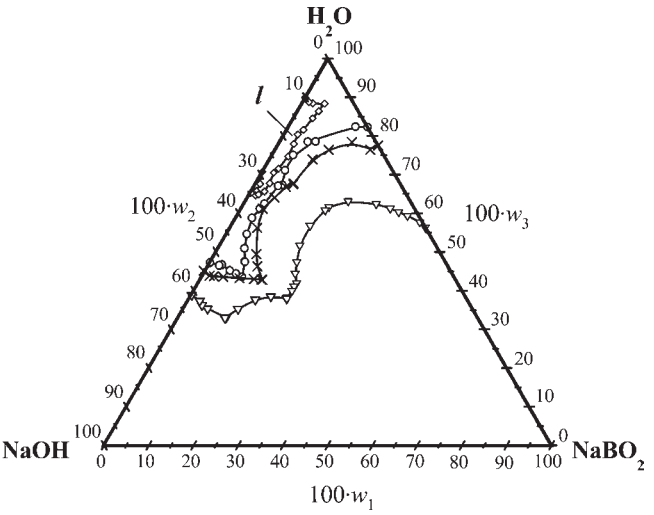

Figure 6. Temperature-induced movement of solubility line for the $NaBO_2$ (1) + KOH (2) + H_2O (3) system: ◇, *t* = −10 °C; ○, *t* = 10 °C; ×, *t* = 25 °C; ▽, *t* = 50 °C. Compositions of equilibrium liquid phase are listed in Tables 2, 3, and 4, and in ref 1.

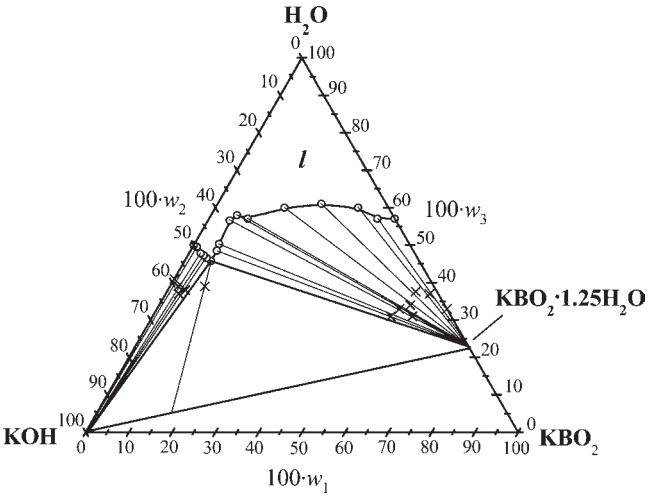

Figure 7. Phase diagram for the KBO_2 (1) + KOH (2) + H_2O (3) system at 10 °C (*l* is the area of the liquid phase). Compositions of equilibrium liquid phase (○) and wet solid phase (+) are listed in Table 5. Thin lines are tie-lines between coexisting phases; thick solid lines are the bounds between monophase, two-phase, and three-phase areas.

on the diagram of the NaOH + $NaBO_2$ + H_2O system at changing temperature.

In similar potassium ternary systems, the temperature-induced transformation of phase diagrams is of some other character. In the potassium systems, the solubility diagram undergoes no essential changes at increases of temperature above 10 °C, whereas in the sodium systems, essential changes in the compositions of solid phases occur at the higher-temperature transition 25 °C → 50 °C. Let us consider key points of the temperature-induced transformation of the diagram of the ternary KBO_2 + KOH + H_2O system.

We examined the component solubility in this ternary system at −10 °C in ref 1. The phase diagram is characterized by the presence of a wide enough homogeneous field and five

dx.doi.org/10.1021/je1007422 |*J. Chem. Eng. Data* 2011, 56, 383–389

Table 5. Equilibrium Data of the KBO_2 + KOH + H_2O System at 10 °C[a]

composition of liquid phase (100 *w*)			composition of wet solid phase (100 *w*)			equilibrium crystalline phase
KBO_2	KOH	H_2O	KBO_2	KOH	H_2O	
43.2	0.0	56.8	67.5	32.5	32.5	$KBO_2 \cdot 1.25H_2O$
38.5	4.2	57.3	61.1	36.9	36.9	$KBO_2 \cdot 1.25H_2O$
32.9	7.3	59.8	—	—	—	$KBO_2 \cdot 1.25H_2O$
23.7	15.5	60.8	58.0	37.0	37.0	$KBO_2 \cdot 1.25H_2O$
15.9	23.6	60.5	57.8	34.5	34.5	$KBO_2 \cdot 1.25H_2O$
8.7	34.3	57.0	56.3	33.1	33.1	$KBO_2 \cdot 1.25H_2O$
6.1	36.2	57.7	—	—	—	$KBO_2 \cdot 1.25H_2O$
5.4	38.2	56.4	59.7	30.9	30.9	$KBO_2 \cdot 1.25H_2O$
5.7	44.0	50.3	—	—	—	$KBO_2 \cdot 1.25H_2O$
6.1	45.4	48.5	55.0	31.0	31.0	$KBO_2 \cdot 1.25H_2O$
6.2	48.1	45.7	8.0	39.0	39.0	KOH + $KBO_2 \cdot 1.25H_2O$ (*e*4)
4.7	48.7	46.6	4.0	38.0	38.0	KOH
3.7	49.0	47.3	3.0	37.0	37.0	KOH
2.7	49.5	47.8	1.8	39.1	39.1	KOH
1.5	49.3	49.2	—	—	—	KOH
0.0	50.0	50.0	0.0	41.0	41.0	KOH

[a] Compositions and the equilibrium crystalline phases of eutonic point (*e*4) are underlined.

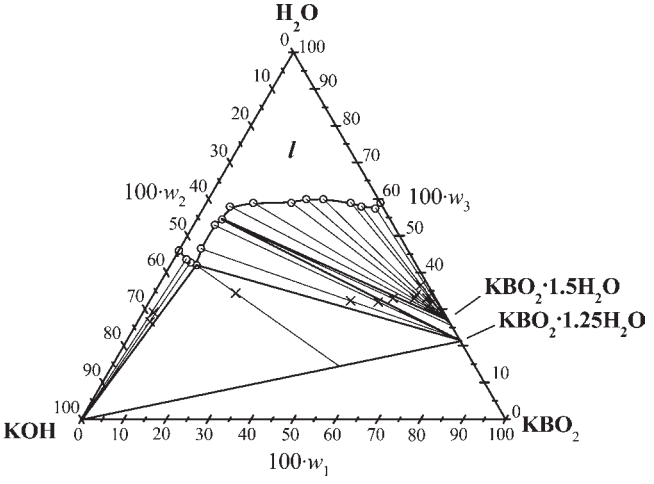

Figure 8. Phase diagram for the KBO_2 (1) + KOH (2) + H_2O (3) system at 25 °C (*l* is the area of the liquid phase). Compositions of equilibrium liquid phase (○) and wet solid phase (+) are listed in the Table 6. Thin lines are tie-lines between coexisting phases; thick solid lines are the bounds between monophase, two-phase, and three-phase areas.

crystallization phases: ice, $KOH \cdot H_2O$, $KBO_2 \cdot 4H_2O$, $KBO_2 \cdot 1.5H_2O$, and $KBO_2 \cdot 1.25H_2O$. When the temperature increases up to +10 °C, the diagram undergoes essential changes, namely, the disappearance of the ice crystallization field and substantial growth of the homogeneous solution area, which is especially valuable from the practical viewpoint (Figure 7). Considering the displacement of the solubility line, note that the total component solubility at movement from the metaborate side of the triangle toward its alkaline one almost does not vary and remains within

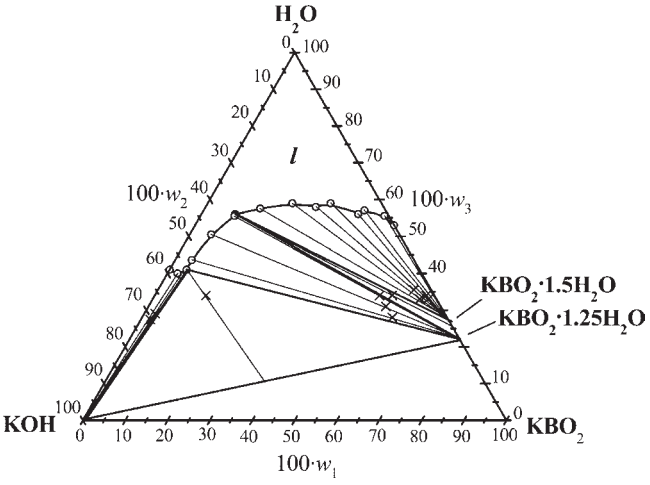

Figure 9. Phase diagram for the KBO_2 (1) + KOH (2) + H_2O (3) system at 50 °C (*l* is area of the liquid phase). Compositions of equilibrium liquid phase (○) and wet solid phase (+) are listed in Table 7. Thin lines are tie-lines between coexisting phases; thick solid lines are the bounds between monophase, two-phase, and three-phase areas.

Table 6. Equilibrium Data of the KBO_2 + KOH + H_2O System at 25 °C[a]

composition of liquid phase (100 *w*)			composition of wet solid phase (100 *w*)			equilibrium crystalline phase
KBO_2	KOH	H_2O	KBO_2	KOH	H_2O	
41.5	0.0	58.5	—	—	—	$KBO_2 \cdot 1.5H_2O$
40.6	2.0	57.4	—	—	—	$KBO_2 \cdot 1.5H_2O$
37.4	4.9	57.7	61.8	1.7	36.5	$KBO_2 \cdot 1.5H_2O$
34.1	6.7	59.2	64.5	2.0	33.5	$KBO_2 \cdot 1.5H_2O$
26.6	13.3	60.1	66.7	2.0	31.3	$KBO_2 \cdot 1.5H_2O$
22.6	17.1	60.3	62.3	3.7	34.0	$KBO_2 \cdot 1.5H_2O$
19.7	20.9	59.4	61.6	5.0	33.4	$KBO_2 \cdot 1.5H_2O$
10.9	30.3	58.8	0.0	0.0	0.0	$KBO_2 \cdot 1.5H_2O$
6.0	36.0	58.0	—	—	—	$KBO_2 \cdot 1.5H_2O$
5.7	39.6	54.7	56.9	9.9	33.2	$KBO_2 \cdot 1.5H_2O$ + $KBO_2 \cdot 1.25H_2O$ (*p*5)
5.2	41.5	53.3	53.6	14.1	32.3	$KBO_2 \cdot 1.25H_2O$
4.9	48.5	46.6	47.3	20.3	32.4	$KBO_2 \cdot 1.25H_2O$
6.2	51.8	42.0	19.4	46.3	34.3	$KBO_2 \cdot 1.25H_2O$ + KOH (*e*5)
4.5	52.8	42.7	3.0	70.5	26.5	KOH
2.8	53.6	43.6	2.5	68.4	29.1	KOH
0.0	53.9	46.1	—	—	—	KOH

[a] Compositions and the equilibrium crystalline phases of peritonic point (*p*5) and eutonic point (*e*5) are underlined.

(0.4 to 0.45) at w_{KOH} = (0 to 0.4). In other words, as much alkali is added to the solution, as much metaborate (approximately) is removed from it. Next, the total solubility grows at the expense of KOH and reaches a maximum at the eutonic point *e*4 where the eutectic contains little metaborate. The compositions of the equilibrium liquid and solid phases are given in Table 5.

In the ternary KBO_2 + KOH + H_2O system at 10 °C, the composition of solid phases has essentially changed as well. By

dx.doi.org/10.1021/je1007422 |*J. Chem. Eng. Data* 2011, 56, 383–389

Table 7. Equilibrium Data of the KBO_2 + KOH + H_2O System at 50 °C[a]

composition of liquid phase (100 *w*)			composition of wet solid phase (100 *w*)			equilibrium crystalline phase
KBO_2	KOH	H_2O	KBO_2	KOH	H_2O	
46.8	0.0	53.2	–	–	–	$KBO_2 \cdot 1.5H_2O$
43.4	1.3	55.3	–	–	–	$KBO_2 \cdot 1.5H_2O$
38.3	4.8	56.9	–	–	–	$KBO_2 \cdot 1.5H_2O$
36.9	6.9	56.2	65.0	2.0	33.0	$KBO_2 \cdot 1.5H_2O$
29.0	12.4	58.6	64.1	1.9	34.0	$KBO_2 \cdot 1.5H_2O$
25.6	16.0	58.4	60.4	4.2	35.5	$KBO_2 \cdot 1.5H_2O$
19.7	21.3	59.0	62.6	4.3	33.1	$KBO_2 \cdot 1.5H_2O$
13.5	29.3	57.2	–	–	–	$KBO_2 \cdot 1.5H_2O$
8.0	36.5	55.5	53.2	12.7	34.1	$KBO_2 \cdot 1.5H_2O$ + $KBO_2 \cdot 1.25H_2O$ (*p*6)
5.1	44.4	50.5	56.4	13.0	30.6	$KBO_2 \cdot 1.25H_2O$
3.7	52.6	43.7	59.0	13.0	28.0	$KBO_2 \cdot 1.25H_2O$
4.3	54.5	41.2	12.0	53.8	34.2	$KBO_2 \cdot 1.25H_2O$ + KOH (*e*6)
3.2	57.2	39.6	2.2	70.4	27.4	KOH
2.4	57.6	40.0	2.5	68.4	29.1	KOH
0.0	58.6	41.4	–	–	–	KOH

[a] Compositions and the equilibrium crystalline phases of peritonic point (*p*6) and eutonic point (*e*6) are underlined.

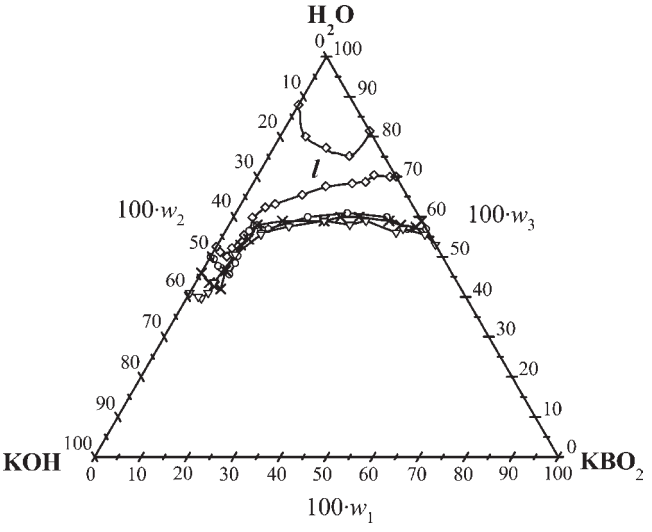

Figure 10. Temperature-induced movement of the solubility line for the KBO_2 (1) + KOH (2) + H_2O (3) system: ◇, *t* = −10 °C; ○ *t* = 10 °C; ×, *t* = 25 °C; ▽, *t* = 50 °C. Compositions of equilibrium liquid phase are listed in Tables 5, 6, and 7, and in ref 1.

using Schreinemakers' technique, the existence of anhydrous KOH and the crystal hydrate $KBO_2 \cdot 1.25H_2O$ has been revealed. Therefore, there is only one eutonic point on the isotherm with no peritonic points. However, this fact does not quite agree with the early phase diagram of the binary KBO_2 + H_2O system,[6] according to which the hydrate $KBO_2 \cdot 1.5H_2O$ should additionally exist at this temperature. We could not find out confidently the existence of $KBO_2 \cdot 1.5H_2O$ in these conditions, but we revealed its existence in the system at *t* = 25 °C.

Increasing the temperature in the KBO_2 + KOH + H_2O system up to 25 °C and up to 50 °C leads to no essential changes in the solubility. The phase diagrams and the compositions of liquid and solid phases are shown in Figures 8 and 9 and in Tables 6 and 7. The eutonic equilibrium is formed by phases ($l + S_{KBO_2 \cdot 1.25H_2O} + S_{KOH}$); the eutonic point *e*5 (*e*6) gradually displaces due to the increase in solubility in the alkaline area of the diagram. The existence of peritonic points *p*5 (*p*6) and three solid phases (KOH, $KBO_2 \cdot 1.25H_2O$, and $KBO_2 \cdot 1.5H_2O$) is a characteristic difference of the ternary system within (25 to 50) °C. Figure 10 summarizes the movement of the solubility line on the triangle of the potassium system at changing temperature. Comparing Figures 6 and 10, one can notice the essentially various characters of temperature influence on the solubility in the $NaBO_2$ + NaOH + H_2O and KBO_2 + KOH + H_2O systems.

CONCLUSION

Concentrated water−alkaline solutions of sodium and potassium borohydrides are used as a fuel and hydrogen source in hydrogen power engineering, including low-temperature fuel cells; borohydrides convert into metaborates. The performance of such mixtures is determined by their component solubility. The solubility in the ternary systems $NaBO_2$ + NaOH + H_2O and KOH + KBO_2 + H_2O was studied by means of isothermal saturation within the range (−10 to 50) °C. The composition of equilibrium solid phases and those of mixtures corresponding to nonvariant equilibrium points were determined; the phase diagrams of these systems were constructed. The presence of a range of homogeneous solutions and fields of crystallization of hydrated and anhydrous forms of the metaborates and hydroxides is characteristic for both systems at all investigated temperatures. The composition of crystalline hydrates depends on the component ratio in the mixture and the cation nature.

Thus, at the −10 °C → +10 °C → 25 °C → 50 °C transition in the ternary KOH + KBO_2 + H_2O system the basic transformations of the compositions of liquid and solid phases take place at lower temperatures within (−10 to +10) °C. A further increase of temperature up to 50 °C renders no significant influence on the solubility of the solid components. The approximate constancy of the total solubility within (0.4 to 0.45) at movements along the solubility line right up to $w_{KOH} \approx 0.4$ is an interesting feature of the system. The weak temperature dependence of solubility is also of value from the practical viewpoint. Besides, in the sodium system a different picture is observed; the solubility of the components and the composition of crystallizing phases vary within the whole temperature range studied [(−10 to 50) °C].

Thus, according to our study, the systems with sodium and potassium ions considerably differ by the temperature influence on the solubility of the solid components. These data have essential importance for FC development with borohydride-type fuel. The high solubility of the BO_2^- ion is important from the viewpoint of avoiding accumulation of the discharge products in the porous structure of FC electrodes. The optimum choice of the component ratio is possible by means of common usage of our phase diagrams.

AUTHOR INFORMATION

Corresponding Author

*Tel.: +7-8452-516413. Fax: +7-8452-271491. E-mail address: churikovav@inbox.ru.

Funding Sources

The authors would like to gratefully acknowledge The Ministry of Education and Science of the Russian Federation for financial support (Contract #P183).

REFERENCES

(1) Churikov, A. V.; Zapsis, K. V.; Khramkov, V. V.; Churikov, M. A.; Smotrov, M. P.; Kazarinov, I. A. Phase Diagrams of Ternary Systems $NaBH_4 + NaOH + H_2O$, $KBH_4 + KOH + H_2O$, $NaBO_2 + NaOH + H_2O$, and $KBO_2 + KOH + H_2O$ at −10 °C. *J. Chem. Eng. Data* **2010**, DOI: 10.1021/je100576m.

(2) Liu, B. H.; Li, Z. P. Current status and progress of direct borohydride fuel cell technology development. *J. Power Sources* **2009**, *187*, 291–297.

(3) Churikov, A. V.; Ivanischev, A. V.; Zapsis, K. V.; Sycheva, V. O.; Gamayunova, I. M. Fuel cells in which used borohydride fuel. *Russ. J. Power Sources* **2009**, *9*, 117–127.

(4) Kim, Ch.; Kim, K. J.; Ha, M. Y. Investigation of the characteristics of a stacked direct borohydride fuel cell for portable applications. *J. Power Sources* **2008**, *180*, 114–121.

(5) Skvorstov, V. G.; Druzhinin, I. G. Polyterm of solubility of the binary systems H_3BO_3 − H_2O, KBO_2 − H_2O and the diagram of fusibility $CO(NH_2)_2$ − H_3BO_3. *Uch. Zap. Chuv. Gos. Pedagog. Inst.* **1969**, *29*, 150–163.

(6) Toledano, P. Equilibrium liquid − solid body in a binary system water − potassium metaborate. *C. R. Acad. Sci.* **1962**, *254*, 2348–2350.

(7) Toledano, P.; Benhassaine, A. Studying of system sodium metaborate − water on the device of a differential thermal analysis under pressure. *C. R. Acad. Sci.* **1970**, *271*, 1577–1580.